



Available online at www.sciencedirect.com



CHAOS
SOLITONS & FRACTALS

Chaos, Solitons and Fractals 26 (2005) 997–1007

www.elsevier.com/locate/chaos

Fractal nature of time series in the sediment transport phenomenon

Pengjian Shang ^{a,*}, Santi Kamae ^b

^a Department of Mathematics, School of Science, Beijing Jiaotong University, Beijing 100044, PR China

^b River and Environmental Engineering Laboratory, Department of Civil Engineering, University of Tokyo, 7-3-1 Hongo, Bunkyo-ku, Tokyo 113-8656, Japan

Accepted 18 January 2005

Abstract

The purpose of the present study is to investigate the presence of fractal behaviors in the sediment transport phenomenon to consider the possibility of using a fractal approach for suspended sediment characterization. Suspended sediment concentration data collected from the Yellow River basin at Tongguan, Shanxi, China are studied. The power spectrum, the empirical probability distribution function, the statistical moment scaling function and the autocorrelation function are used as indicators to investigate the presence of fractal. The results from the fractal identification methods indicate that the sediment data exhibit fractal behavior.

© 2005 Elsevier Ltd. All rights reserved.

1. Introduction

Hydrological processes, such as suspended sediment, are usually non-linear, complex, dynamic and widely scattered due to the influence physical process involved and the variability in space and time [1–3,5,9–11,13,18,22,24,25,31]. The underlying complexity and variability make suspended sediment investigation one of the elusive tasks in hydrology. However, adequate knowledge of the sediment transport phenomenon in rivers is needed for studies of reservoir sedimentation, river morphology, soil and water conservation planning, water quality modeling and design of efficient erosion control structures. There are many physical components forming the sediment transport system and the mechanisms involved in the dynamics of the process. As such components and the mechanisms involved act on a range of temporal and spatial scales, understanding their individual dynamics and their (independent and/or combined) influence on the overall sediment transport phenomenon is non-trivial. The problem becomes more complicated, since these components and the mechanisms involved, in turn, not only depend on a host of other factors, such as climatic conditions, basin characteristics, etc., but also exhibit varying degrees of non-linearity. In this regard, the notion of deterministic chaos, that seemingly complex irregular behavior could be the result of simple deterministic systems influenced by a few dominant non-linear interdependent variables with sensitive dependence on initial conditions, may provide potential alternatives.

* Corresponding author.

E-mail addresses: pjshang@center.njtu.edu.cn (P. Shang), santi@hydra.t.u-tokyo.ac.jp (S. Kamae).

Research on the investigation of the existence of a chaos in the sediment transport phenomenon has gained considerable attention in recent times [1,3,9,10,12,13,15,18,25,30,31]. The outcomes of such studies, on the one hand, nearly unanimously indicated the presence of a chaos nature in the sediment transport phenomenon. On the other hand, most of the studies have also revealed the insufficiency of the chaos approaches to characterize the hydrological process. These papers were motivated by a hypothesis that the sediment transport systems are often chaotic. The difficulty with this hypothesis is that chaos theory presumes system determinism. Since the sediment transport system involve climatic conditions, basin characteristics, and other possibly (probably?) random agents, such an assumption is not easy to justify. Thus, chaos theory may not well apply. Also, while chaos may exist on a small level, it may be neither discernable nor of (apparent) practical significance. This raises the issue of the usefulness of chaos theory to practitioners. This has led researchers to employ the fractal approaches directly, even without verifying the possibility of fractal in the hydrological process [4,6–8,16,19–21,23,26–29,34,36,37]. A possible explanation for this may be that most of the fractal approaches, such as the power spectrum method, could indicate whether the hydrological process exhibits a fractal nature.

The theoretical basis of fractal approaches for the sediment transport phenomenon is the assumption that the variability of the hydrological process could be directly modeled as a stochastic (or random) turbulent cascade process [19–21,28,33,35,38]. A cascade process is generally described as eddies breaking up into smaller sub-eddies, each of which receives a part of the flux of its parent body. The above assumption is supported by the empirical evidence about the fractal properties of the hydrological process and the analogy with the stochastic cascade models in fully developed turbulence. It is important to note, however, that though there have been several attempts to justify their applicability to the hydrological process by an analogy with the energy cascade process in the fully developed turbulence, such stochastic cascade approaches are purely phenomenological. Therefore, whether or not the sediment transport phenomenon is stochastic cascade remains an unanswered question. Nevertheless, the following are the possible reasons for the validity of stochastic fractal approaches for the sediment transport phenomenon: (1) the belief that the hydrological process and the breaking-up of eddies are stochastic; and (2) stochastic cascade processes generically yield fractals.

The purpose of the present study is to investigate the presence of fractal behaviors in the sediment transport phenomenon so as to investigate the possibility of a fractal approach. The suspended sediment concentration data observed over a period of about 31 years from the Yellow River basin at Tongguan, Shanxi, China are analyzed, and the study deals with the fractal analyses only in time. The existence of fractal is investigated by employing four methods: (1) the power spectrum; (2) the empirical probability distribution function; (3) the statistical moment scaling function; and (4) the autocorrelation function method, which is employed to investigate the existence of long-range dependence and self-similarity, specified in terms of a Hurst parameter, in the sediment transport phenomenon.

The organization of this paper is as follows. First, a brief review of the methods employed in the present study to identify the presence of fractals in a time series is given in Section 2. Details of the data used, analyses carried out and results achieved are presented in Section 3. Finally, important conclusions drawn from this study are provided in Section 4.

2. Proposed methodology

Research over the past two decades has led to the development of a wide variety of methods to identify fractals in a time series. However, before applying any fractal identification method, general information about the fractal behavior may be obtained by using standard statistical descriptions, such as the power spectrum and the empirical probability distribution function. These two methods are, therefore, employed in the present study. In addition, the statistical moment scaling function can provide important information regarding the existence of a fractal and its type, whether mono-fractal or multi-fractal, and, therefore, is also employed. Finally, the autocorrelation function method is employed to investigate the existence of long-range dependence and self-similarity in the sediment transport phenomenon. In this section, a brief account of these four methods is provided.

2.1. Power spectrum

The power spectrum is a standard tool in fractal investigations in hydrological process [7,17,26]. When all or part of the spectrum obeys the power law form

$$E(f) \propto f^{-\delta} \quad (1)$$

where f is the frequency and δ is an exponent, called the spectral exponent, the data are scaling in that range, that is, the scaling regime. The absence of characteristic timescales indicates that fractal behavior may be assumed to hold. Also, the power spectrum is particularly useful for studying the oscillations of a process. In general, for a random process, the

power spectrum oscillates randomly about a constant value, indicating that no frequency explains any more of the variance of the sequence than any other frequency. For a periodic or quasi-periodic sequence, only peaks at certain frequencies exist; measurement noise adds a continuous floor to the spectrum. Thus, in the spectrum, signal and noise are readily distinguished. Chaotic signals may also have sharp spectral lines, but even in the absence of noise there will be a continuous part of the spectrum.

2.2. Empirical probability distribution function

The empirical probability distribution function (PDF) of a time series describes the fractal of the intensity thresholds of the time series fluctuations at a given scale, generally the scale corresponding to the measurement resolution. If, for high-intensity threshold values x , the tail of the probability distribution of the time series X follows a power law of form

$$\Pr(X > x) \propto x^{-D} \quad (2)$$

where D is the probability exponent, then the series is characterized by hyperbolic intermittency [19]. This is a general, but not necessary, feature of multi-fractal processes [7]. In fact, a value of $D < 2$ indicates that mono-fractal models may be sufficient to characterize the hydrological phenomenon, whereas multiplicative (and generally multi-fractal) models are necessary if $D > 2$ [19,37]. From (2) it can be deduced that moments of order greater or equal to D are divergent.

2.3. Statistical moment scaling method

To investigate the scaling behavior of the time series, the variation of empirical moments with scale is examined. This analysis is a common technique to study scaling properties of hydrological data and has been applied to rainfall time series by, for example, Over and Gupta [28]. Among the existing multi-fractal identification methods, the statistical moment scaling method [8,28,33] is the most widely used one in hydrography. In this method, the time series is divided into non-overlapping intervals of a certain time resolution. The ratio of the maximum scale of the field to this interval is termed the ‘scale ratio’ k . Thus k is inversely proportional to the size of the scale examined. For different scale ratios k , the average intensity $\varepsilon(k, i)$, in each interval i is computed and raised to power q , and subsequently summed to obtain the statistical moment $M(k, q)$:

$$M(k, q) = \sum_i \varepsilon(k, i)^q \quad (3)$$

Since values of $\varepsilon(k, i) = 0$ do not contribute to the moment, and these terms are undefined when raised to $q = 0$, they were excluded from the computation. For a scaling field, the moment $M(k, q)$ relates to the scale ratio k , as

$$M(k, q) = k^{\theta(q)} \quad (4)$$

where $\theta(q)$ may be regarded as a characteristic function of the fractal behavior. If $\theta(q)$ versus q is a straight line the data set is mono-fractal. On the other hand, if $\theta(q)$ versus q is a convex function, the data set is multi-fractal [8,34].

2.4. Autocorrelation function

The autocorrelation function is useful in determining the degree of dependence present in the values of a time series, separated by an interval called lag time τ . In general, the autocorrelation function of a random process fluctuates about zero, indicating that the process at any instance of time has no memory of the past at all. The autocorrelation function of a periodic process is also periodic, indicating the strong relation between values that repeat over and over again. For a chaotic process, the autocorrelation function decays exponentially with increasing lag, because the points are not independent of each other and self-similarity is present. As a rule, a delay in the autocorrelation function indicates a temporal persistence that may also be related to fractal properties of the time series [32].

A phenomenon that is self-similar looks the same or behaves the same when viewed at different degrees of “magnification” or different scales on a dimension. This dimension may be space (length, width) or time. In the following, we give a brief account of the methods employed in the present study to identify the presence of self-similarity in a time series.

Let $X = (X_t; t = 1, 2, \dots)$ be a covariance stationary stochastic process; that is a process with constant mean $\mu = E(X_t)$, finite variance $\sigma^2 = E[(X_t - \mu)^2] > 0$, and an autocorrelation function

$$R(\tau) = \frac{E[(X_t - \mu)(X_{t+\tau} - \mu)]}{E[(X_t - \mu)^2]}, \quad \tau = 0, 1, 2, \dots \quad (5)$$

Let us assume that X has an autocorrelation function of the form

$$R(\tau) \sim \tau^{-\beta} L_1(\tau), \quad \tau \rightarrow \infty \quad (6)$$

where $0 < \beta < 1$ and L_1 is slowly varying at infinity, that is, $\lim_{t \rightarrow \infty} L_1(tx)/L_1(t) = 1$ for all $x > 0$. For each $m = 1, 2, \dots$, let

$$X^{(m)} = (X_k^{(m)}; k = 1, 2, \dots)$$

denote a new time series obtained by averaging the original series X over non-overlapping blocks of size m . That is, for each $m = 1, 2, \dots, X^{(m)}$ is given by

$$X_k^{(m)} = \frac{X_{km-m+1} + \dots + X_{km}}{m}, \quad k = 1, 2, \dots \quad (7)$$

The process X is called (exactly second order) self-similar with self-similarity parameter $H = 1 - \beta/2$ if the corresponding aggregated processes $X^{(m)}$ have the same correlation structure, i.e.

$$R^{(m)}(\tau) = R(\tau), \quad m = 1, 2, \dots, \quad \tau = 1, 2, \dots \quad (8)$$

X is called (asymptotically second order) self-similar with self-similarity parameter $H = 1 - \beta/2$ if

$$R^{(m)}(1) \rightarrow 2^{1-\beta} - 1, \quad m \rightarrow \infty$$

$$R^{(m)}(\tau) \rightarrow \frac{1}{2}\delta^2(\tau^{2-\beta}), \quad \tau = 2, 3, \dots, \quad m \rightarrow \infty$$

where $\delta^2(g)$ denotes the second central difference operator applied to a function g [39].

Self-similarity is the property we associate with fractals—the object appears the same regardless of the scale at which it is viewed. It is manifested in the absence of a natural length of a “burst”; at every time scale ranging from a few hours to days and months, bursts consisting of bursty sub-periods separated by less bursty sub-periods.

The degree of self-similarity, defined via the Hurst parameter H , can be used to measure the “burstiness” of the sediment transport phenomenon. As H increases the degree of self-similarity is increasing ($0.5 < H < 1$). For $H = 0.5$ and $H > 1$, there is almost no self-similarity.

A stochastic process satisfying relation (6) is said to exhibit long-range dependence [39]. Processes with long-range dependence are characterized by an autocorrelation function that decays hyperbolically. Hyperbolic decay is much slower than exponential decay, and since $\beta < 1$, the sum of the autocorrelation values of such series approaches infinity. The implication of this non-summable autocorrelation is that, if we consider n samples from the series, then the variance does not decrease as a function of “ n ” but by a value of $n^{-\beta}$.

The Hurst parameter can be derived from β in the above equation from the relation $H = 1 - \beta/2$. Note that H is always in the range $0 < H < 1$. The Hurst parameter is an important measure of long-range dependence. If $H = 1/2$ then a data set has independent data—an example of such a data set would be Brownian motion where points in the time series depend only on their nearest neighbor. If $H > 1/2$ then the data set has long-range dependence. That is (in loose terms) data which is spatially separated in the series is likely to be correlated. If $H < 1/2$ then the data set has negative long-range dependence, that is to say, in loose terms data which is spatially separated in the series is likely to have a negative correlation [39].

3. Results and analyses

3.1. The suspended sediment data at Tongguan, Shanxi, China

Sediment data from the Yellow River basin at Tongguan, Shanxi, China are studied. The Yellow River, originating from the Yueguzonglie basin on the northern part of the Bayankela Mountain in Tibet highlands situated at an elevation of 4500 m is flowing through nine provinces, with a total length of 5464 km, basin area 795,000 km² and, finally empties itself into the Bohai Sea. It is the second largest river in China, and downstream being protected area of 120,000 km² from flooding. The total population within river basin is 107 million; the cultivated land is 12 million ha.

With regard to sediment transport, the Yellow River transports more sediment than any other river in China. In spite of the large dams that have been built across its major tributaries, the Yellow River still ranks first in the China in suspended sediment discharge to the Bohai sea. The average annual suspended sediment discharge to the coastal zone by the Yellow River is about 1.6 billion ton with suspended sediment concentration 35 kg/m³. Every year, average 400 million tons of sediment deposit on the lower reach of the Yellow River, which results in rising of river bed with a speed of 10 cm. The river channel of downstream is 4–7 m higher than the ground outside the river on average; the maximum is up to 13 m higher.

The sediment data in the Yellow River basin are measured at a number of stations throughout the basin. For the present study, data collected in the Tongguan station of the Yellow River basin are used. The natural flow of the stream at the gauging station is affected by many reservoirs and navigation dams in the upper Yellow River basin and by many diversions for irrigation in the Yellow River basin.

Even though daily sediment and discharge data measurements have been made available from May 1950 for the above station, there were some missing data before 1968 and also after 1998. Although a longer record is always desirable for hydrological investigations, it is also important to have continuous data, particularly in studies such as this, where the objective is to investigate the changes in the system with time (i.e. dynamics). The use of continuous data would obviously eliminate the potential uncertainties (on data quality and hence the outcomes of the methods employed) that could arise from interpolation and other schemes if the record were to contain missing data. For the same reason, it was decided to consider only a particular period when data are continuously available. Therefore, data observed over a period of 31 years, from January 1968 to December 1998, are considered. Also, time series of only one component involved in the sediment transport phenomenon, namely suspended sediment concentration, is studied. The variations of this time series are shown in Fig. 1.

Fig. 1 shows the time series plot of the suspended sediment concentration values observed at Tongguan, Shanxi, China. A visual inspection of the suspended sediment series only indicates significant variations in sediment concentration, but this is not enough to say anything regarding the existence of fractals. Hence, additional tools are necessary to identify the possible presence of fractals.

3.2. Power spectrum

We now attempt to empirically estimate the scaling ranges of the observed suspended sediment time series. This is conveniently done by calculating the power spectrum $E(f)$ (in one dimension, ensemble average of the square of the Fourier amplitudes as a function of the frequency f) and estimating the spectral exponent δ in the scaling relation $E(f) \propto f^{-\delta}$. Although the spectrum is defined as an ensemble average quantity, if the series is long enough, it may be possible to get some idea of the scaling range and exponent on individual realizations.

The power spectrum of a time series, through the spectral exponent δ , can be used to obtain important information regarding the cascade that results in a process, in addition to identifying the presence or absence of characteristic time scales, i.e. a fractal nature. For instance, a necessary, but not sufficient, condition for the process to be a direct result of an unbounded cascade is that $\delta < 1$.

Fig. 2 shows the power spectrum $E(f)$ of the suspended sediment time series, in the range 2 days to 31 years, observed at Tongguan, Shanxi, China. The spectrum has been averaged over logarithmically spaced frequency intervals. The

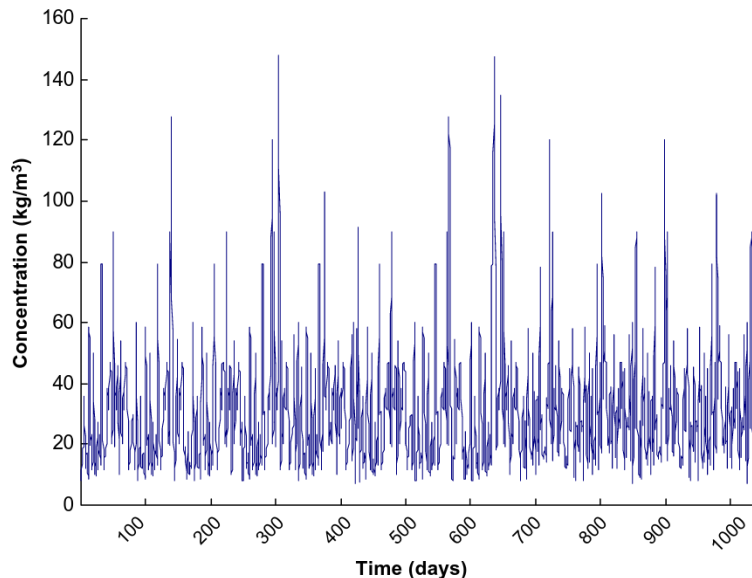


Fig. 1. Variation of daily suspended sediment concentration in the Yellow River at Tongguan, Shanxi, China.

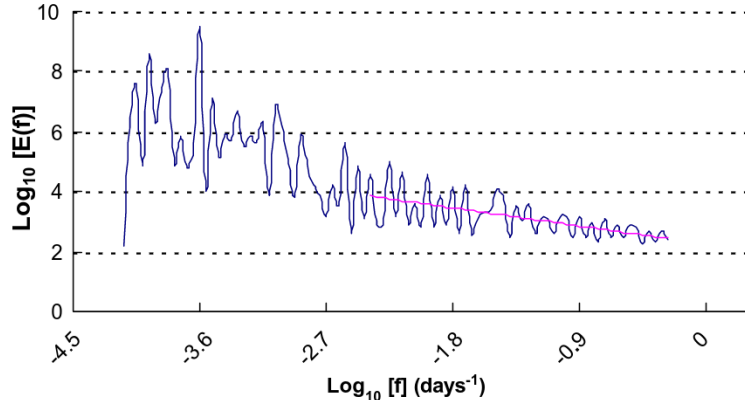


Fig. 2. Power spectrum for daily sediment data from Tongguan, Shanxi, China. (For interpretation of the references in color in this figure legend, the reader is referred to the web version of this article.)

spectrum appears to consist of a power law interval in the range 2 days to 360 days. But the straight-line approximation may be extended up to 370 days with a reasonable fit (the red, straight regression line) with $\delta = 0.72$. The presence of a scaling regime, shown by the red line in Fig. 2, may be considered as an indication of fractal behavior. The value of δ , calculated from the slope of the red line, is approximately 0.72 and, therefore, an unbounded cascade model may be sufficient to represent the sediment transport process. It should be noted, however, that the identification of the scaling regime(s) and the estimation of the spectral exponent(s) depend on individual judgment and, therefore, discrepancies and uncertainties are unavoidable. As a result, extreme caution is needed while using the power spectrum to identify the existence of fractals in a time series. Similarly, the power spectrum shown in Fig. 2 is not sufficient to identify whether the sediment transport process is chaotic or stochastic, as chaotic processes may also show a continuous part of the spectrum even in the absence of noise.

3.3. Probability distribution function

The empirical PDF obtained for the suspended sediment time series observed at Tongguan, Shanxi, China is shown in Fig. 3. The figure shows that the suspended sediment data exhibit a hyperbolic tail behavior with a probability exponent D , estimated from the fitted regression line, of about 2.6. Since the D value obtained for the suspended sediment time series is greater than 2, a mono-fractal model is not sufficient to model the sediment transport phenomenon [19,37], as it cannot accommodate a value of $D > 2$. This suggests that a multi-fractal model, which can accommodate any value of D , is necessary to model the sediment transport phenomenon observed at Tongguan, Shanxi, China. To our great surprise, the D value obtained is approximate to the ones obtained by past studies for daily rainfall observed at other regions [17,34,37].

3.4. Statistical moment scaling method

In this method, the suspended sediment intensity is averaged over successively doubled time intervals corresponding to successively halved values of the scale ratio k , and for each k the q th statistical moment is calculated according to Eq. (3). By plotting $M(k, q)$ as a function of k in a log-log diagram, the scaling behavior of the time series as expressed by Eq. (4) may be investigated. If Eq. (4) is valid the curve will exhibit an approximately linear behavior with a slope that is an estimate of $\theta(q)$. By performing the procedure for different values of q , the whole $\theta(q)$ function may be estimated. Owing to uncertainties in the estimation of high-order moments, the investigation is limited to orders in the range $0 \leq q \leq 3.9$. Fig. 4 shows the $M(k, q)$ as a function of k in a log-log diagram for the suspended sediment time series observed at Tongguan, Shanxi, China, for $0 \leq q \leq 3.9$. The curves in Fig. 4 exhibit a well-defined straight-line behavior over the whole scaling regime for $q \leq 2.7$. However, the moments of higher order do not follow a straight line for the time series. The disruption of the linearity of the curve for $q > 3$ coincides with the D value from the empirical probability distribution ($D = 2.6$, in Fig. 3). Also, it can be noted that the higher the order of the moment, the less linear the character of $M(k, q)$ is.

The relationship between $\theta(q)$ and q is shown in Fig. 5. Function of $\theta(q)$ was estimated from the sloped of the fitted regression line for the suspended sediment time series. The $\theta(q)$ function is shown for moment orders up to 3 for the

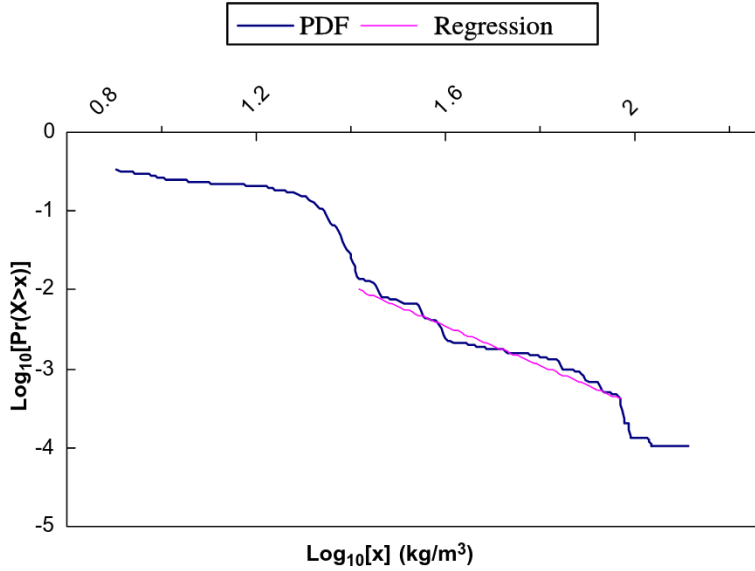


Fig. 3. Empirical probability distribution function, $\text{Pr}(X>x)$, for daily sediment data from Tongguan, Shanxi, China. (For interpretation of the references in color in this figure legend, the reader is referred to the web version of this article.)

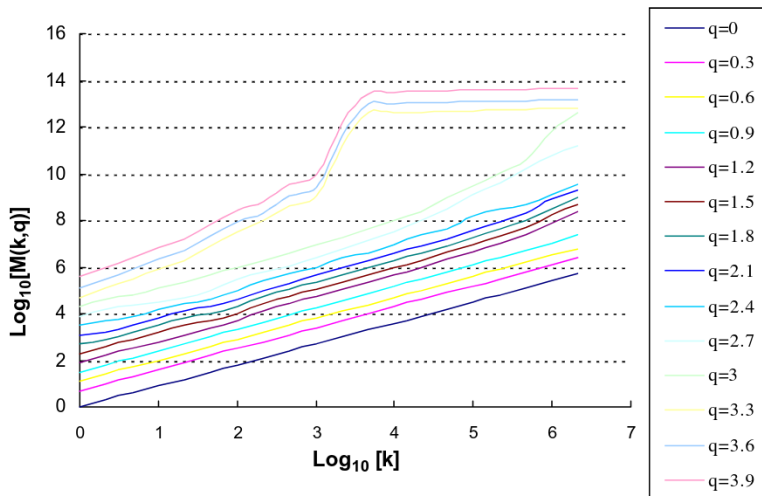


Fig. 4. The q th statistical moment, $M(k,q)$, as a function of the scale ratio, q , in the scaling regime for daily sediment data from Tongguan, Shanxi, China. (For interpretation of the references in color in this figure legend, the reader is referred to the web version of this article.)

time series. As seen in the figure, the $\theta(q)$ versus q function is a convex curvature, rather than a straight line, indicating that the suspended sediment data are multi-fractal. The $\theta(q)$ function is slightly curved for $0 \leq q < 3$ but becomes more linear as q increases.

3.5. Autocorrelation function

Fig. 6 shows the variation of the autocorrelation function against the lag time for the suspended sediment time series observed at Tongguan, Shanxi, China. The autocorrelation function indicates a lag time of about 6 days. The delay in the autocorrelation function, though small, may be due to the presence of chaotic dynamics in the sediment transport

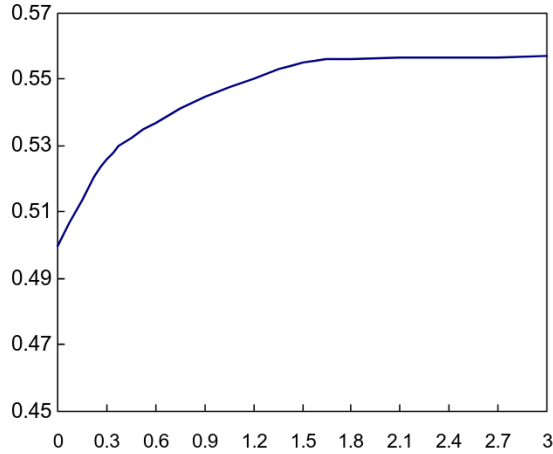


Fig. 5. Estimated $\theta(q)$ function for daily sediment data from Tongguan, Shanxi, China.

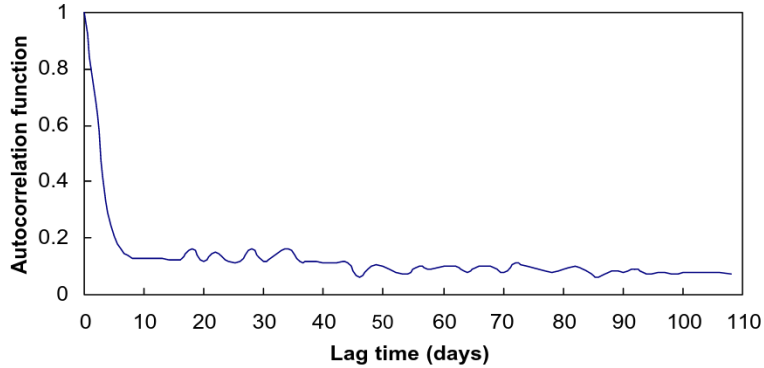


Fig. 6. Autocorrelation function $R(\tau)$ for daily sediment data from Tongguan, Shanxi, China.

phenomenon. The delay in the autocorrelation function may also be interpreted to show temporal persistence and, hence, be considered related to a fractal nature [32]. However, one has to be cautious while using the autocorrelation function for distinguishing between stochastic and chaotic processes. For instance, a rapid fall in the autocorrelation function is normally considered as an indication of a stochastic process, but even chaotic processes, such as the Hénon map [14], yield rapid falls in the autocorrelation function. These observations indicate that the autocorrelation function is neither a necessary nor a sufficient indicator to characterize a process, chaotic or stochastic, or fractal or non-fractal.

If a self-similar process has observable bursts on all time scales, it is said to exhibit long-range dependence [39]; values at any instant are typically correlated with value at all future instants. The existence of long-range dependence can be seen from Fig. 6, which decays very slowly, indicating significant correlations, even over large delays (0.1 for $\tau = 100$).

Several methods [39] are commonly used for measuring the long-range dependence of the sediment transport phenomenon. We shall mention two important ones here, R/S plots and variance time plots.

First we deal with R/S plots. Let X_k : $k = 1, 2, \dots, n$, be a set of n observations which have an expectation value (sample mean) $E[X(n)]$, the scaled, adjusted range is given by

$$\frac{R(n)}{S(n)} = \frac{\max(0, W_1, \dots, W_n) - \min(0, W_1, \dots, W_n)}{S(n)}$$

where $S(n)$ is the standard deviation and for each $k: 1, 2, \dots, n$, W_k is given by

$$W_k = (X_1 + X_2 + \dots + X_k) - kE[X(n)], \quad k = 1, 2, \dots, n$$

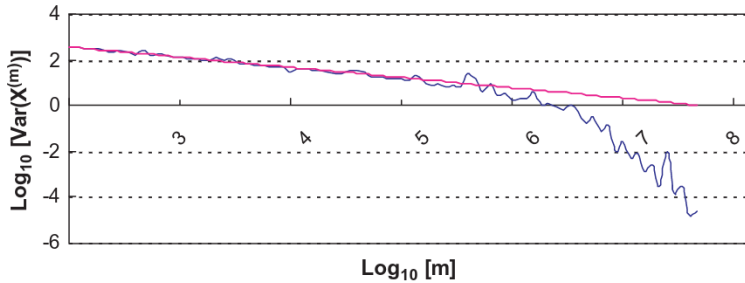


Fig. 7. The variance-time plot for daily sediment data from Tongguan, Shanxi, China. (For interpretation of the references in color in this figure legend, the reader is referred to the web version of this article.)

The Hurst parameter is given by the equation: $R(n)/S(n) \sim cn^H$. By taking logs we get:

$$\log_{10}(R(n)/S(n)) \sim \log_{10}c + H\log_{10}n$$

Therefore the gradient of a plot of $\log_{10}(R/S)$ against $\log_{10}n$ is the Hurst parameter.

A second method for calculation is a variance time plot. Again, let X_k be a series of observations for $k = 1, 2, \dots, n$. If we take a sample of m points, $\text{Var}[X^{(m)}] \sim m^{-\beta}$. Therefore, the gradient of a plot of $\log_{10}[\text{Var}(X^{(m)})]$ against $\log_{10}m$ will be $-\beta$ and the Hurst parameter can be found using the equation $H = 1 - \beta/2$.

We give here the variance time plots (Fig. 7) for the suspended sediment time series observed at Tongguan, Shanxi, China. The curve shows an asymptotic slope that is distinctly different from -1 and is easily estimated to be about -0.38 resulting in an estimate \hat{H} of the Hurst parameter H of about $\hat{H} = 0.81$.

4. Conclusion

Applications of the ideas gained from fractal theory to characterize hydrological processes have been one of the most exciting areas of research in recent times. This paper presented a detailed analysis of fractal properties of the suspended sediment time series. The data stemmed from measurements collected over a period of 31 years (January 1968 to December 1998) at Tongguan, Shanxi, China. Our analysis aimed to examine whether this data possesses any fractal structure or whether it has rather a stochastic character. The existence of a fractal nature was investigated using the power spectrum, the empirical probability distribution function, the statistical moment scaling methods, and the autocorrelation function, which is employed to investigate the existence of self-similarity and long-range dependence, specified in terms of a Hurst parameter, in the sediment transport phenomenon.

The presence of a scaling regime in the power spectrum of the suspended sediment time series indicated the possibility of fractal behavior. The value of the spectral exponent δ was approximately 0.72 and, being less than unity, suggests that an unbounded cascade model might be sufficient. The results of the empirical probability distribution function analysis, with probability exponent $D > 2$, indicated the insufficiency of a mono-fractal model and the need for a multi-fractal model to characterize the sediment transport phenomenon. The observation of a convex curvature, rather than a straight line, of the statistical moment scaling function indicated that the suspended sediment data analyzed exhibited multi-fractal properties. The delay observed, though small, in the autocorrelation function could be an indication of the presence of chaotic dynamics in the sediment transport phenomenon, and could be interpreted to show temporal persistence, which might also be related to a fractal nature. We found strong evidence, the Hurst parameter $H = 0.81$, of a long-range dependence, which was not accounted for in any of the commonly used stochastic models for the sediment transport phenomenon. This can serve as one ground for using this model in the hydrological processes.

The above results from the present investigation provided positive evidence regarding the existence of fractal behavior in the suspended sediment data from Tongguan, Shanxi, China. A possible implication of this might be that suspended sediment characterization could be viewed from a new perspective: the chaotic fractal perspective. It should be noted, however, that the methods employed in the present study possess inherent limitations. For example, insufficient data size and the presence of noise may influence the outcomes of the fractal identification methods [11]. Therefore, the results obtained here should be substantiated further using other fractal and chaos identification methods to provide strong proof regarding the existence of a fractal and chaotic nature in the sediment transport phenomenon. Investigations in these directions are under way, details of which will be reported elsewhere.

Acknowledgments

The authors thank Chinese Hydraulic Institute (CHI) for providing the daily sediment data in the Yellow River. Pengjian Shang was partially supported by the funds of Beijing Jiaotong University (2003SM006).

References

- [1] Bhutiyani MR. Sediment load characteristics of a proglacial stream of Siachen Glacier and the erosion rate in Nubra valley in the Karakoram Himalayas, India. *J Hydrol* 2000;227:84–92.
- [2] Bull LJ. Relative velocities of discharge and sediment waves for the River Severn, UK. *Hydrol Sci J* 1997;42(5):649–60.
- [3] Bull LJ, Lawler DM, Leeks GJL, Marks S. Downstream changes in suspended sediment fluxes in the River Severn, UK. In: Osterkamp WR, editor. Effects of scale on interpretation and management of sediment and water quality. Proc Boulder Symp, IAHS Pub no 226, July 1995. p. 27–36.
- [4] de Lima MIP, Grasman G. Multifractal analysis of 15-min and daily rainfall from a semi-arid region in Portugal. *J Hydrol* 1999;220:1–11.
- [5] Einstein HA. Formulas for the transportation of bedload. *J Hydraul Div ASCE* 1943;107:561–97.
- [6] Fraedrich K. Estimating the dimensions of weather and climate attractors. *J Atmos Sci* 1986;43(5):419–32.
- [7] Fraedrich K, Larnder C. Scaling regimes of composite rainfall time series. *Tellus* 1993;45A:289–98.
- [8] Frisch U, Parisi G. On the singularity structure of fully developed turbulence. In: Ghil M, Benzi R, Parisi G, editors. Turbulence and predictability in geophysical fluid dynamics and climate dynamics. New York: North-Holland; 1985. p. 84–8.
- [9] Gilvear DJ. Suspended solids transport within regulated rivers experiencing periodic reservoir releases. In: Craig JF, Kemper JB, editors. Regulated rivers: advances in ecology. London, UK: Plenum; 1987. p. 245–55.
- [10] Gilvear DJ, Petts GE. Turbidity and suspended solids variation downstream of a regulating reservoir. *Earth Surf Proces Land* 1985;10:363–73.
- [11] Harris D, Seed A, Menabde M, Austin G. Factors affecting multiscaling analysis of rainfall time series. *Nonlin Process Geophys* 1997;4:137–55.
- [12] Hasnain SI. Factors controlling suspended sediment transport in Himalayan glacier meltwaters. *J Hydrol* 1996;181:49–62.
- [13] Heidel SG. The progressive lag of sediment concentration with flood waves. *Trans Am Geophys Union* 1956;37:56–66.
- [14] Henon M. A two-dimensional mapping with a strange attractor. *Commun Math Phys* 1976;50:69–77.
- [15] Hilborn, Robert C. Chaos and nonlinear dynamics: an introduction for scientists and engineers. 2nd ed. Oxford: Oxford University Press; 2001.
- [16] Krasovskaya I, Gottschalk L, Kundzewicz ZW. Dimensionality of scandinavian river flow regimes. *Hydrol Sci J* 1999;44(5):705–23.
- [17] Ladoy P, Lovejoy S, Schertzer D. Extreme variability of climatological data: scaling and intermittency. In: Schertzer D, Lovejoy S, editors. Non-linear variability in geophysics. Norwell, MA: Kluwer Academic; 1991. p. 241–50.
- [18] Leeks GJL, Newson MD. Responses of the sediment system of regulated river to a scour valve release: Llyn Clywedog, Mid Wales, UK. *Regul Rivers* 1989;3:93–6.
- [19] Lovejoy S, Mandelbrot B. Fractal properties of rain and a fractal model. *Tellus* 1985;37A:209–32.
- [20] Lovejoy S, Schertzer D. Multifractals, universality classes and satellite and radar measurements of clouds and rain fields. *J Geophys Res* 1990;95(D3):2021–34.
- [21] Lovejoy S, Schertzer D. Multifractals and rain. In: Kundzewicz ZW, editor. New uncertainty concepts in hydrology and hydrological modeling. New York: Cambridge University Press; 1995. p. 61–103.
- [22] Meade RH, Parker RS. Sediment in rivers of the United States. National water summary 1984—hydrologic events, selected water quality trends, and groundwater resources. US Geological Survey Water Supply Paper 2275, 1985. p. 1–467.
- [23] Menabde M, Harris D, Seed A, Austin G, Stow D. Multiscaling properties of rainfall and bounded random cascades. *Water Resour Res* 1997;33(12):2823–30.
- [24] Milliman JD, Meade RH. World wide delivery of river sediments to the oceans. *J Geol* 1983;91:1–9.
- [25] Olive LJ, Olley JM, Wallbrink PJ, Murray AS. Downstream patterns of sediment transport during floods in the Murrumbidgee River, NSW, Australia. *Z Geomorphol* 1996;105(Supplementband):129–40.
- [26] Olsson J, Niemczynowicz J, Berndtsson R. Fractal analysis of high-resolution rainfall time series. *J Geophys Res* 1993;98(D12):23265–74.
- [27] Osborne AR, Provenzale A. Finite correlation dimension for stochastic systems with power-law spectra. *Physica D* 1989;35:357–81.
- [28] Over TM, Gupta VK. Statistical analysis of mesoscale rainfall: dependence of a random cascade generator on large-scaling forcing. *J Appl Meteorol* 1994;33:1526–42.
- [29] Porporato A, Ridolfi L. Nonlinear analysis of river flow time sequences. *Water Resour Res* 1997;33(6):1353–67.
- [30] Restrepo JD, Kjerfve B. Magdalena river: interannual variability (1975–1995) and revised water discharge and sediment load estimates. *J Hydrol* 2000;235:137–49.
- [31] River Severn UK. In: Osterkamp WR, editor. Effects of scale on interpretation and management of sediment and water quality. Proc Boulder Symp, July 27–36, IAHS Publ no 226, 1995.

- [32] Rodriguez-Iturbe I, De Power FB, Sharifi MB, Georgakakos KP. Chaos in rainfall. *Water Resour Res* 1989;25(7):1667–75.
- [33] Schertzer D, Lovejoy S. Physical modeling and analysis of rain and clouds by anisotropic scaling multiplicative processes. *J Geophys Res* 1987;92(D8):9693–714.
- [34] Svensson C, Olsson J, Berndtsson R. Multifractal properties of daily rainfall in two different climates. *Water Resour Res* 1996;32(8):2463–72.
- [35] Takens F. Detecting strange attractors in turbulence. In: Rand DA, Young LS, editors. *Dynamical systems and turbulence. Lecture notes in mathematics*, vol. 898. Berlin: Springer-Verlag; 1981. p. 366–81.
- [36] Tessier Y, Lovejoy S, Hubert P, Schertzer D, Pecknold S. Multifractal analysis and modeling of rainfall and river flows and scaling, causal transfer functions. *J Geophys Res* 1996;101(D21):26427–40.
- [37] Tessier Y, Lovejoy S, Schertzer D. Universal multifractals: theory and observations for rain and clouds. *J Appl Meteorol* 1993;32:223–50.
- [38] Weidlich, Wolfgang. *Sociodynamics: a systematic approach to mathematical modeling in the social sciences*. Amsterdam: Harwood Academic; 2000.
- [39] Willinger W, Taqqu MS, Sherman W, Wilson D. Self-similarity through high variability: statistical analysis of Ethernet LAN traffic at the source level. *IEEE/ACM Trans Network* 1997;5(1):71–86.